Research Article

Mathematical Methods in the Applied Sciences

Received XXXX

(www.interscience.wiley.com) DOI: 10.1002/sim.0000
MOS subject classification: 37G15; 34K40

Mathematical modeling of tumor surface growth with necrotic kernels

Hua Zhang[a], Jianjun Paul Tian[b], Ben Niu[c*†], Yuxiao Guo[c]

A two-dimensional tumor-immune model with the time delay of the adaptive immune response is considered in this paper. The model is designed to account for the interaction between cytotoxic T lymphocytes (CTLs) and cancer cells on the surface of a solid tumor. The model considers the surface growth as a major growth pattern of solid tumors in order to describe the existence of necrotic kernels. We conduct detailed qualitative analyses. The system has three equilibria. Both zero and maximum tumor volume equilibria are unstable, while the behavior of the positive equilibrium is closely related to the ratio of the immune killing rate to tumor volume growth rate. The positive equilibrium is more likely to be locally asymptotically stable when the ratio is smaller than a critical value, and unstable otherwise. The analysis about the distribution of eigenvalues yields conditions to guarantee the existence of Hopf bifurcation at the positive equilibrium. Applying the center manifold reduction and normal form method, we obtain explicit formulas to determine the properties of Hopf bifurcations. The global continuation of local Hopf bifurcation is investigated based on the coincidence degree theory. The results reveal that the time of the adaptive immune system taking to response to tumors can lead to oscillation dynamics. We also carry out detailed numerical analysis for parameters and numerical simulations to illustrate our qualitative analysis. Numerically, we find that a shorter immune response time leads to a longer patient survival time and the period and amplitude of a stable periodic solution increase with the immune response time. When CTLs recruitment rate and death rate vary, we observe how the ratio of the immune killing rate to tumor volume growth rate and the first bifurcation value of the immune response time change numerically, which yields further insights to the tumor-immune dynamics.

Keywords: tumor-immune model; surface contact; stability; Hopf bifurcation; global continuation

1. Introduction

Cancer, an unnatural growth phenomenon of cell numbers, remains mostly intractable disease despite the fact that tremendous advances have been made in treatment techniques and medicine ([1, 2]). Finding effective strategies for tumor control and therapies is significant for public health, as well as for economic resources. However, it is a great challenge since the growth and control of tumors involve a considerable number of biological mechanisms and dynamical processes that are too complicated to be fully captured. As studies of complexities in physics, tumor-associated responses can be better approached by establishing mathematical models with some appropriate simplified assumptions than via experimental procedures alone ([3, 4, 5, 6]).

Tumor immunology, over the last two decades, has attracted remarkable attention and various mathematical models have been developed to understand the interaction between cancer and immune cells. A review of early works concerning tumor-immune system interaction can be found in [7, 8]. Given the complexity of this process, many models include four or more variables or equations. For example, Kuznetsov et al. ([9]) proposed a system with five equations to investigate the mediated response to growing tumor mass, which can be applied to the tumor dormancy. However, in order to better recognise the main response mechanism between immune cells and tumor mass, some simplifications are excepted. As in [10], authors presented a coupled ordinary equation system to account for the role of cytotoxic T lymphocytes (CTLs) in solid tumors growth, where CTLs can recognize and kill the cancer cells in a tumor, recruit other immune cells to the tumor site ([11]). The structure of a tumor in

[a] *Department of Mathematics, Harbin Institute of Technology, Harbin, Heilongjiang 150001, China*
[b] *Department of Mathematical Sciences, New Mexico State University, New Mexico, USA*
[c] *Department of Mathematics, Harbin Institute of Technology, Weihai, Shandong 264209, China*
[*] *Correspondence to: Ben Niu, Department of Mathematics, Harbin Institute of Technology, Weihai, Shandong 264209, China.*
[†] E-mail: niu@hit.edu.cn

Prepared using mmaauth.cls [Version: 2009/09/02 v2.00]

[10] was supposed to be a sphere with a inner shell representing a necrotic kernel, and the active cellular division only occurred on the surface of the tumor sphere, which is shown in Figure 1. Similar idea was also proposed in [12].

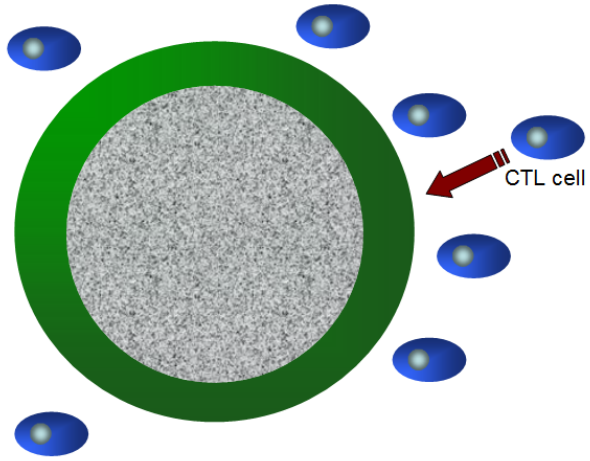

Figure 1. A tumor with a necrotic kernel and surface tumor-immune interaction.

It is well-known that there are two immune systems, the innate immune system and adaptive immune system, and they have different response dynamics in cancer immune interactions ([13]). The innate immune response functions as the first line of defence against infection. It consists of soluble factors, such as complement proteins, and diverse cellular components including granulocytes (basophils, eosinophils and neutrophils), mast cells, macrophages, dendritic cells and natural killer cells. The adaptive immune response is slower to develop, but manifests as increased antigenic specificity and memory. It consists of antibodies, B cells, and CD4+ and CD8+ T lymphocytes. Natural killer T cells and $\gamma\delta$ T cells are cytotoxic lymphocytes that straddle the interface of innate and adaptive immunity ([14]). Clearly, the adaptive immune system takes some time to response to cancer cell growth. CTLs belong to the adaptive immune system. To appropriately model CTLs-mediated immune response to tumor cells, the time delay of the adaptive immune response should not be ignored. Besides, numerous results, such as [15, 16, 17] have demonstrated that the time delay can produce rich dynamics in a system, such as the stability switches and periodic oscillations. [15] incorporated three delays required for tumor cells proliferation, effector cells growth and the immune effector cells differentiation and obtained stable interval of every delay.

A solid tumor grows from a slow avascular growth period due to the nutrient limitation. Interested by the CTLs-mediated immune response on this stage, the authors in [10] proposed the following model:

$$\begin{cases} \dot{V}(t) = \rho r_t V^{2/3}(t) - \rho k V^{2/3}(t) C(t), \\ \dot{N}(t) = \rho r_c V^{2/3}(t) N(t) - d_c N(t). \end{cases} \tag{1.1}$$

Here, $V(t)$ and $N(t)$ stand for the volume of the tumor mass and the number of CTLs with ability to attack the tumor cells at time t, respectively. It is assumed that the tumor has a spherical shape and the radius changes when tumor grows. So the tumor surface area is proportional to $\rho V^{2/3}(t)$, where ρ is the dimensionless shape factor changing with the tumor volume. r_c is the CTLs' recruitment rate and r_t is the growth rate of tumor volume. The death rate of CTLs is denoted by d_c and the rate at which cancer cells are killed by CTLs is k. A dimensionless function, $C(t)$, was introduced to stand for the fraction of the attacked surface area. All parameters in system (1.1) are positive.

Note that the term $V^{2/3}(t)N(t)$ is a functional response with fractional powers. This type of response functions has been widely used (see [18, 19, 20] and references therein). The authors in [20] proposed that it was better to use surface area than volume when modeling the prey in groups. They further verified that the fractional term significantly affected the existence of interior equilibrium and periodic solutions. The authors in [18] presented stable oscillations induced by time delay as well pointed out that small fractional orders was better for system to remain stable.

The logistic function is one common choice for model species growth. Thus, in this paper, we use it to describe the growth of tumor in the absence of CTLs. In addition, the Holling II response function is used to model tumor-CTLs interaction. It is more practical to use a discrete time delay to reflect the time for the adaptive immune system to response to the tumor. Accordingly, we propose a two-compartment model as

$$\begin{cases} \frac{dT(t)}{dt} = rT^{2/3}(t)\left[1 - \frac{T(t)}{T_m}\right] - kT^{2/3}(t)\frac{N(t)}{N(t)+\beta}, \\ \frac{dN(t)}{dt} = \rho T^{2/3}(t-\tau)N(t-\tau) - dN^2(t), \end{cases} \tag{1.2}$$

where r is the growth rate of the tumor, T_m is the maximum volume of a tumor, d stands for the death rate of the CTLs, and ρ is the recruitment rate of CTLs. The parameters k is defined as that in model (1.1). The last term in the second equation indicates that the death of CTLs is nonlinear ([21]). The parameters and their values are summarized in Table 1.1.

Table 1.1. Common ranges and units for parameters in system (1.2)

Parameter	Description	Biological ranges and unit	Reference
ρ	CTLs' recruitment rate	$0-0.48\ day^{-1}$	[22]
r	Tumor's growth rate	$0-0.33\ day^{-1}$	[23]
k	CTLs' killing rate for tumor	$0-0.9\ day^{-1}$	[24]
d	CTLs' death rate	$0-0.38\ day^{-1}$	[23]

The main goal of this paper is to study the effect of adaptive immune response delay on the stability of system (1.2). In particular, we intend to seek some conditions such that system (1.2) undergoes Hopf bifurcation at positive equilibrium induced by delay. We are further going to analyse the properties of bifurcating periodic solutions in local and global range. In fact, the center manifold method and normal form theory presented by [25, 26] are two useful tools for this problem and they have been applied by many literatures (see [27, 30] and many others). Biologically, the Hopf bifurcation phenomenon implies that the tumor and CTLs interaction in a periodical fashion, and the tumor mass can never be eradicated. It is also noticed that when the time required by CTLs to response to the tumor is less than branching value, the tumor and CTLs can coexist, which implies the tumor can be controlled. Moreover, following the global Hopf bifurcation theory given in [28], we verify the global continuation of local Hopf bifurcation. Understanding how the parameters in model, especially the delay τ, affect the solutions is helpful for successful treatment.

The rest of this paper is organized as follows. In Section 2, we investigate the existence and stability of equilibria, establish the conditions for Hopf bifurcations, and obtain explicit formulas to determine the direction of Hopf bifurcation and the stability of the periodic solutions. In Section 3, we discuss the global existence of Hopf bifurcation. In Section 4, we carry out some numerical simulations to illustrate our analytical results and exhibit the effects of other parameters in model on the bifurcation parameter. Finally, we give a brief conclusion in the last section.

2. Basic analysis

In this section, we provide basic analysis, such as the local stability of trivial and boundary equilibria, existence of positive equilibrium and its local stability. Moreover, the properties of Hopf bifurcation occurring at positive equilibrium are demonstrated.

2.1. Local stability of trivial and boundary equilibria

Clearly, the system (1.2) always has two equilibria: $E_0 = (0, 0)$ and $E_1 = (T_m, 0)$. Due to the term of $T^{2/3}$, the local stability of E_0 cannot be obtained by the distribution of corresponding eigenvalues. In order to remove fractional power, it is common to rescale T by $T = x^3$. However, such a rescalling cannot cover the dynamics near E_0. Motivated by [19], we assume $0 \le T(\theta),\ N(\theta) \le \delta,\ \theta \in [-\tau, 0]$ for a sufficiently small constant $0 < \delta \ll 1$. Then around the origin, the system becomes

$$\begin{cases} \dfrac{\mathrm{d}T(t)}{\mathrm{d}t} \approx rT^{2/3}(t), \\ \dfrac{\mathrm{d}N(t)}{\mathrm{d}t} \approx \rho T^{2/3}(t-\tau)N(t-\tau). \end{cases} \tag{2.1}$$

This implies $\frac{\mathrm{d}T(0)}{\mathrm{d}t} > 0$, $\frac{\mathrm{d}N(0)}{\mathrm{d}t} > 0$. Following from the continuity of $T(t)$ and $N(t)$ near the origin, $T(t)$ and $N(t)$ both increase with respect to t around E_0. Therefore, the solutions of system (1.2) initiating from a small neighborhood of E_0 ultimately depart from it. Thus, E_0 is always unstable.

In the following, the boundary equilibrium E_1 is analysed. For simplification, a new variable $x(t) = T^{1/3}(t)$ is introduced, and the substitution is

$$\begin{cases} \dot{x}(t) = \dfrac{r}{3}\left[1 - \dfrac{x^3(t)}{T_m}\right] - \dfrac{k}{3}\dfrac{N(t)}{\beta + N(t)}, \\ \dot{N}(t) = \rho x^2(t-\tau)N(t-\tau) - dN^2(t). \end{cases} \tag{2.2}$$

Further, make the following dimensionless: $x(t) = T_m^{1/3}\hat{x}(t)$, $N(t) = \beta\hat{N}(t)$, $\hat{r} = \frac{r}{3}T_m^{-1/3}$, $\hat{k} = \frac{k}{3}T_m^{-1/3}$, $\hat{\rho} = \rho T_m^{2/3}$, $\hat{d} = d\beta$ and drop the hats, then system (2.2) is converted to

$$\begin{cases} \dot{x}(t) = r[1 - x^3(t)] - k\dfrac{N(t)}{1 + N(t)}, \\ \dot{N}(t) = \rho x^2(t-\tau)N(t-\tau) - dN^2(t). \end{cases} \tag{2.3}$$

The boundary equilibrium $(T_m, 0)$ becomes $(1, 0)$. It is easy to get that the characteristic equation of the linearization associated with system (2.3) at $(1, 0)$ is

$$(\lambda + 3r)(\lambda - \rho e^{-\lambda\tau}) = 0. \tag{2.4}$$

Apparently, the stability of $(1,0)$ depends on roots of

$$\lambda - \rho e^{-\lambda\tau} = 0. \tag{2.5}$$

In the case of $\tau = 0$, it can be solved $\lambda = \rho > 0$, which implies $(1,0)$ is unstable; For $\tau > 0$, we can check that $\lambda = 0$ is not a root of Eq. (2.5), moreover, although $\lambda = i\rho$ is a root of Eq. (2.5) at $\tau = \tau_k = \frac{1}{\rho}\left(\frac{\pi}{2} + 2k\pi\right)$, $k = 1, 2, \ldots$ but $\mathrm{Re}\left(\frac{\mathrm{d}\lambda(\tau)}{\mathrm{d}\tau}\right)\Big|_{\tau=\tau_k} = 0$, thus, $(1,0)$ keeps unstable. Consequently, $(T_m, 0)$ is unstable.

Summarizing the discussions above, we state the stability of E_0 and E_1 in the following theorem.

Theorem 2.1 *For system (1.2), the trivial equilibrium E_0 and boundary equilibrium E_1 are both unstable.*

Remark 2.1 *It's clear that the ideal case that tumor doesn't appear in the body and the worst case that adaptive immune system doesn't work and tumor grows to it's maximum volume are easily effected by external factors.*

2.2. Existence and local stability of positive equilibrium

We next turn to the coexistence state of CTLs and tumor. Note that the possible positive equilibrium (T_*, N_*) of system (1.2) becomes $E_* = (x_*, N_*)$ of system (2.3) after the transformation above. Further, the system (2.3) has identical dynamics with the system (1.2) at E_*, thus, we only need to consider system (2.3) in later discussions.

Some trivial calculations give the existence and uniqueness of positive equilibrium E_*.

Lemma 2.1 *System (2.3) always has a unique positive equilibrium $E_* = (x_*, N_*)$ with $N_* = \frac{\rho x_*^2}{d}$ and x_* being the positive solution of $\rho x^5 + dx^3 - \rho(1 - \frac{k}{r})x^2 - d = 0$.*

Proof Assume that (x, N) is a positive solution for system (2.3). It is easy to get $N = \frac{\rho x^2}{d}$ from the second equation of system (2.3). Substituting it into the first equation, we have

$$\rho x^5 + dx^3 - \rho(1 - \frac{k}{r})x^2 - d = 0. \tag{2.6}$$

Denote

$$H(x) = \rho x^5 + dx^3 - \rho(1 - \frac{k}{r})x^2 - d. \tag{2.7}$$

Taking derivatives of both sides of equation (2.7) with respect to x yields

$$H'(x) = 5\rho x^4 + 3dx^2 - 2\rho(1 - \frac{k}{r})x. \tag{2.8}$$

Case I: If $1 - \frac{k}{r} \le 0$, obviously, $H'(x) \ge 0$ for $x \ge 0$. Furthermore, $H(0) = -d < 0$, and $\lim_{x\to\infty} H(x) = \infty$, which implies that $H(x) = 0$ has a unique solution for $x \in (0, \infty)$;

Case II: If $1 - \frac{k}{r} > 0$, let $G(x) = 5\rho x^3 + 3dx - 2\rho(1 - \frac{k}{r})$. Thus, $H'(x) = xG(x)$. Since $G'(x) > 0$, $G(0) < 0$ and $\lim_{x\to\infty} G(x) = \infty$, there is a unique root for $G(x) = 0$, we set it as x_1. Hence, $H'(x) < 0$ for $x \in (0, x_1)$; $H'(x) \ge 0$ when $x > x_1$. We also notice that $H(x_1) < H(0) = -d < 0$ and $\lim_{x\to\infty} H(x) = \infty$. Thus, there exists a unique zero for $H(x) = 0$ when $x \in (x_1, \infty)$. The proof is completed. □

Linearizing system (2.3) at E_* leads to

$$\begin{cases} \dot{x}(t) = -3rx_*^2 x(t) - \dfrac{k}{(1+N_*)^2} N(t), \\ \dot{N}(t) = -2dN_* N(t) + 2\rho x_* N_* x(t-\tau) + \rho x_*^2 N(t-\tau). \end{cases} \tag{2.9}$$

The corresponding characteristic equation of (2.9) is

$$\lambda^2 + A\lambda + B + (C\lambda + D)e^{-\lambda\tau} = 0, \tag{2.10}$$

with $A = 2dN_* + 3rx_*^2$, $B = 6rdx_*^2 N_*$, $C = -\rho x_*^2$, $D = \frac{2\rho k x_* N_*}{(1+N_*)^2} - 3r\rho x_*^4$.

Naturally, we have the following result describing the stability of E_* in the case of $\tau = 0$.

Theorem 2.2 *E_* is locally asymptotically stable for $\tau = 0$.*

Proof When $\tau = 0$, the Eq.(2.10) becomes

$$\lambda^2 + (A + C)\lambda + (B + D) = 0. \tag{2.11}$$

It can be easily verified that

$$A + C = (\rho + 3r)x_*^2 > 0, \quad B + D = 3r\rho x_*^4 + \frac{2\rho k x_* N_*}{(1 + N_*)^2} > 0.$$

The Routh-Hurwitz criterion shows that all characteristic roots of Eq.(2.11) have negative real parts. The proof is completed. □

For $\tau > 0$, let $i\omega$ $(\omega > 0)$ be a root of (2.10), then we have

$$-\omega^2 + iA\omega + B + (iC\omega + D)e^{-i\omega\tau} = 0.$$

Separating the real and imaginary parts gives

$$\begin{aligned} D\cos\omega\tau + C\omega\sin\omega\tau &= \omega^2 - B, \\ D\sin\omega\tau - C\omega\cos\omega\tau &= A\omega. \end{aligned}$$

Adding the square of both sides of above two equations yields

$$\omega^4 + (A^2 - C^2 - 2B)\omega^2 + (B^2 - D^2) = 0,$$

and

$$\omega^2 = \frac{C^2 + 2B - A^2 \pm \sqrt{(A^2 - C^2 - 2B)^2 - 4(B^2 - D^2)}}{2}.$$

According to the expressions of A, B and C, we have

$$A^2 - C^2 - 2B = (2dN_* + 3rx_*^2)^2 - \rho^2 x_*^4 + 12rdx_*^2 N_* = 3\rho^2 x_*^4 + 9rx_*^4 > 0.$$

Assume

$$(H_1): \qquad B < D$$

is satisfied, then we obtain

$$\omega_0 = \frac{\sqrt{2}}{2}\sqrt{C^2 - A^2 + 2B + \sqrt{(C^2 - A^2 + 2B)^2 - 4(B^2 - D^2)}}. \tag{2.12}$$

Further, we can derive that

$$\tau_j = \begin{cases} \dfrac{1}{\omega_0}\left[\arccos\dfrac{D(\omega_0^2 - B) - AC\omega_0^2}{C^2\omega_0^2 + D^2} + 2j\pi\right], & \cos\omega_0\tau > 0, \\ \dfrac{1}{\omega_0}\left[\pi - \arccos\left(-\dfrac{D(\omega_0^2 - B) - AC\omega_0^2}{C^2\omega_0^2 + D^2}\right) + 2j\pi\right], & \cos\omega_0\tau < 0, \ j = 0, 1, 2.... \end{cases} \tag{2.13}$$

Let $\lambda = \alpha(\tau) + i\omega(\tau)$ be a root of (2.10) satisfying $\alpha(\tau_j) = 0$ and $\omega(\tau_j) = \omega_0$. Some calculations yield the following result.

Lemma 2.2 *If the assumption* (H_1) *holds, then* $\mathrm{Re}\left(\frac{\mathrm{d}\lambda}{\mathrm{d}\tau}\right)|_{\tau=\tau_j} > 0$.

Proof Differentiating both sides of (2.10) with respect to τ gives

$$\frac{\mathrm{d}\lambda(\tau)}{\mathrm{d}\tau} = \frac{(C\lambda + D)\lambda}{(2\lambda + A)e^{\lambda\tau} + C - (C\lambda + D)\tau}.$$

It follows that,

$$\left[\frac{\mathrm{dRe}(\lambda(\tau))}{\mathrm{d}\tau}\right]^{-1} = \mathrm{Re}\left[\frac{(2\lambda + A)e^{\lambda\tau} + C}{(C\lambda + D)\lambda}\right],$$

then we obtain

$$\begin{aligned} \left[\frac{\mathrm{dRe}(\lambda(\tau))}{\mathrm{d}\tau}\right]^{-1}|_{\tau=\tau_j} &= \frac{D\omega_0(A\sin\omega_0\tau_j + 2\omega_0\cos\omega_0\tau_j) - C\omega_0^2(A\cos\omega_0\tau_j - 2\omega_0\cos\omega_0\tau_j + C)}{C^2\omega^4 + D^2\omega^2} \\ &= \frac{A^2 - C^2 - 2B + 2\omega_0^2}{C^2\omega_0^2 + D^2}. \end{aligned}$$

Again, using $A^2 - C^2 - 2B > 0$, we have $\frac{A^2 - C^2 - 2B + 2\omega_0^2}{C^2\omega_0^2 + D^2} > 0$, which completes the proof. □

According to the results in [29, 30], we arrive at the following results.

Lemma 2.3 *For system (2.3), we have*
(i) *If assumption* (H_1) *is not satisfied, then all roots of Eq.(2.10) have negative real parts for all* $\tau \geq 0$;
(ii) *If* (H_1) *holds, then we can find a sequence of values of* τ: $0 < \tau_0 < \tau_1 < \cdots < \tau_j < \cdots$ *such that all eigenvalues have negative real parts when* $\tau \in [0, \tau_0)$; *Eq.(2.10) has* $2(j+1)$ *roots with positive real parts when* $\tau \in (\tau_j, \tau_{j+1}], j = 0, 1, 2, ...$; *For* $\tau = \tau_j$, $j = 0, 1, 2, ...$, *Eq.(2.10) has exactly a pair of simple imaginary roots* $\pm i\omega_0$.

Now, based on the fundamental Hopf bifurcation theorem in [31], we have the following stability results at E_* and the existence of Hopf bifurcations.

Theorem 2.3 *For system (2.3), the following results hold true.*
(i) *Assume* (H_1) *is not satisfied, the positive equilibrium* E_* *is locally asymptotically stable for* $\tau \geq 0$;
(ii) *Assume* (H_1) *holds true, then* E_* *is locally asymptotically stable for* $\tau \in [0, \tau_0)$ *and unstable for* $\tau > \tau_0$. *Furthermore, a Hopf bifurcation takes place at* E_* *when* $\tau = \tau_j, j = 0, 1, 2, ...$

Remark 2.2 *Noticing that all results obtained above are closely related to* (H_1), *thus, we a give brief discussion about it.*
Denote (x, N) *be the positive equilibrium of (2.3), then we have* $N = \rho x^2/d$. *By the expressions of* B *and* D, *we have*

$$B - D = \rho r x^3 \Big[9x - \frac{2\rho d\frac{k}{r}}{(d+\rho x^2)^2}\Big]$$

Clearly, $B - D$ *is monotone increasing with respect to* x. *Meanwhile,* $\max\Big\{0, \Big(1-\frac{k}{r}\Big)^{1/3}\Big\} < x < 1$ *is satisfied. As a result, if* $\frac{k}{r} \leq 1$, *we have*

$$\begin{aligned}\rho r x^3\Big[9x(d+\rho x^2)^2 - 2\rho d\frac{k}{r}\Big] &> 9\rho r\Big(1-\frac{k}{r}\Big)^{4/3}\Big[d+\rho\Big(1-\frac{k}{r}\Big)^{2/3}\Big]^2,\\ &> 0,\end{aligned}$$

which means $B > D$ *always holds when* $\frac{k}{r} \leq 1$. *In fact, we also know* $B < D$ *implies* $\frac{k}{r} > 1$. *In terms of biology, when the CTLs killing rate is less than tumor growth rate, the tumor is stable and will not be easily influenced by some external factors. In later study, we will give some numerical simulations to illustrate how other factors impact* (H_1) *and the existence of Hopf bifurcation on* $k - r$ *plane.*

2.3. Properties of Hopf bifurcation

In the previous subsection, we have obtained a sufficient condition to guarantee system (2.3) to undergo Hopf bifurcations. According to the center manifold theorem, we know that the projection of periodic solution bifurcating from the first bifurcation value τ_0 on the center manifold has the same stability with that of system (2.3). Therefore, we shall study the direction of Hopf bifurcation and the stability of bifurcating periodic solutions with the center manifold theory and normal form method given in [25]. The details will be provided in Appendix, and the consequence is stated as the following theorem.

Theorem 2.4 *Suppose that the assumption* (H_1) *is satisfied. In the neighborhood of the bifurcation value, the Hopf bifurcation at* E_* *is supercritical (subcritical) if* $\mathrm{Re}(c_1(0)) < 0$ (> 0).

The expression of $c_1(0)$ is deduced in Appendix, we shall carry out some numerical simulations to illustrate our theoretical analysis in section 4.

3. Global existence of periodic solutions

In this section, we always assume all solutions of system (2.3) are nonnegative and (H_1) is true, and consider the global existence of Hopf bifurcation at the point $(E_*, \tau_j), j = 0, 1, 2, ...$, by applying the global bifurcation result developed by [28].

Let $\mathbb{R}^2_+ = \{(x, N) \in \mathbb{R}^2, x > 0, N > 0\}$, $\mathcal{C} = C([-\tau, 0], \mathbb{R}^2_+)$ and $v_t = (x_t, N_t) \in \mathcal{C}$ with $v_t(\theta) = v(t+\theta)$ for $t \geq 0$, $\theta \in [-\tau, 0]$. System (2.3) can be abstracted as the following functional differential equation

$$\dot{v}(t) = F(v_t, \tau, s) \tag{3.1}$$

where

$$F(\Psi, \tau, s) = \begin{pmatrix} r(1-\psi_1^3(0)) - \frac{k\psi_2(0)}{1+\psi_2(0)} \\ \rho\psi_1^2(-\tau)\psi_2(-\tau) - d\psi_2^2(0)\end{pmatrix},$$

and $\Psi = (\psi_1, \psi_2) \in \mathcal{C}$. The mapping $F : \mathcal{C} \times \mathbb{R}_+ \times \mathbb{R}_+ \to \mathbb{R}^2_+$ is completely continuous. To restrict F onto the subspace of $\mathcal{C}$ composed by all constant functions, we define the mapping $\hat{F} = F\,|_{\mathbb{R}^2_+\times\mathbb{R}_+\times\mathbb{R}_+} : \mathbb{R}^2_+ \times \mathbb{R}_+ \times \mathbb{R}_+ \to \mathbb{R}^2_+$. Obviously,

$$\hat{F}(v, \tau, s) = \begin{pmatrix} r(1-x^3) - \frac{kN}{1+N} \\ \rho x^2 N - dN^2\end{pmatrix}. \tag{3.2}$$

Denote constant mapping $v_0 \in \mathcal{C}$ by v^*. The point (v^*, τ^*, s^*) is said to be a stationary solution of (3.1) if $\hat{F}(v^*, \tau^*, s^*) = 0$. Therefore, we get

(A1) $\hat{F} \in \mathcal{C}^2(\mathbb{R}^2_+ \times \mathbb{R}_+ \times \mathbb{R}_+, \mathbb{R}^2_+)$.

Furthermore, under assumption (H_1), we have

$$\det(D_v \hat{F}(v, \tau, s) \mid_{v=v^*}) = \det \begin{pmatrix} -3x_*^2 & -\frac{k}{(1+N_*)^2} \\ 2\rho x_* N_* & \rho x_*^2 - 2dN_* \end{pmatrix} < 0.$$

Thus, we have

(A2) $D_v \hat{F}(v, \tau, s)$ at the positive equilibrium v^* is an isomorphism on $\mathbb{R}^2_+$;

It is also clearly that

(A3) $F(\Psi, \tau, s)$ is differentiable with respect to Ψ.

At any stationary solution (v^*, τ^*, s^*), the corresponding characteristic matrix is

$$\Delta(v^*, \tau^*, s^*)(\lambda) = \lambda \mathrm{I} - D_\Psi F(v^*, \tau^*, s^*)(e^{\lambda \cdot} \mathrm{I}),$$

namely,

$$\Delta(v^*, \tau^*, s^*)(\lambda) = \begin{pmatrix} \lambda + 3x_*^2 & \frac{k}{(1+N_*)^2} \\ -2\rho x_* N_* e^{-\lambda\tau} & \lambda - \rho x_*^2 e^{-\lambda\tau} + 2dN_* \end{pmatrix},$$

then we obtain that

$$\det(\Delta(v^*, \tau^*, s^*)(\lambda)) = \lambda^2 + A\lambda + B + (C\lambda + D)e^{-\lambda\tau}, \tag{3.3}$$

where A, B, C, D are defined as in (2.10).

The stationary solution (v^*, τ^*, s^*) is called a center if

$$\det\Big(\Delta(v^*, \tau^*, s^*)\big(n\frac{2\pi i}{s}\big)\Big) = 0$$

for some integer n. A center (v^*, τ^*, s^*) is said to be isolated if it is the only center in some neighborhood of (v^*, τ^*, s^*). It can be easily verified that $\Big(v^*, \tau_j, \frac{2\pi}{\omega_0}\Big), j = 0, 1, 2, \ldots$ are isolate centers based on the analysis in section 2. We also know that there exist $\eta > 0$, $\xi > 0$ and a smooth curve $\lambda : (\tau_j - \eta, \tau_j + \eta) \to \mathbb{C}$, such that

$$\det(\Delta(v^*, \tau^*, s^*)(\lambda(\tau))) = 0, \tag{3.4}$$

$\mid \lambda(\tau) - i\omega_0 \mid < \xi$ for all $\tau \in [\tau_j - \eta, \tau_j + \eta]$ and $\lambda(\tau_j) = i\omega_0$, $\frac{\mathrm{dRe}(\lambda)}{\mathrm{d}\tau} \mid_{\tau=\tau_j} > 0$.

Define

$$\Omega_{\xi, \frac{2\pi}{\omega_0}} = \left\{(u, s) : 0 < u < \xi, \mid s - \frac{2\pi}{\omega_0} \mid < \xi\right\}.$$

Then the following hypotheses can be proved on $(\tau_j - \eta, \tau_j + \eta) \times \Omega_{\xi, \frac{2\pi}{\omega_0}}$.

(A4) $\det\Big(\Delta(v^*, \tau^*, s^*)\big(u + i\frac{2\pi}{s}\big)\Big) = 0$ if and only if $u = 0, \tau = \tau_j$ and $s = \frac{2\pi}{\omega_0}$, $j = 0, 1, 2, \ldots$.

In what follows, we define

$$\Sigma(F) = \mathrm{Cl}\{(v, \tau, s) \in \mathbb{C} \times \mathbb{R}_+ \times \mathbb{R}_+ : v_{t+s} = u_t\},$$
$$N(F) = \{(v^*, \tau, s) \in \mathbb{R}^2_+ \times \mathbb{R}_+ \times \mathbb{R}_+ : F(v^*, \tau, s) = 0\},$$

and let $D\Big(v^*, \tau_j, \frac{2\pi}{\omega_0}\Big)$ be the connected component for the center $\Big(v^*, \tau_j, \frac{2\pi}{\omega_0}\Big)$ of (3.1) in $\Sigma(F)$. Then the following lemma holds.

Lemma 3.1 *$D\Big(v^*, \tau_j, \frac{2\pi}{\omega_0}\Big)$ is unbounded for each center $\Big(v^*, \tau_j, \frac{2\pi}{\omega_0}\Big)$.*

Proof As in [28], we define

$$\mathcal{H}^{\pm}\Big(v^*, \tau_j, \frac{2\pi}{\omega_0}\Big)(u, s) = \det\Big(\Delta\Big(v^*, \tau_j \pm \eta, \frac{2\pi}{\omega_0}\Big)\Big(u + i\frac{2\pi}{s}\Big)\Big).$$

Assumption (A4) indicates that $\mathcal{H}^{\pm}\Big(v^*, \tau_j, \frac{2\pi}{\omega_0}\Big)(u, s) \neq 0$ for $(u, s) \in \Omega_{\xi, \frac{2\pi}{\omega_0}}$, then the first crossing number $\gamma\Big(v^*, \tau_j, \frac{2\pi}{\omega_0}\Big)$ is

$$\begin{aligned} \gamma\Big(v^*, \tau_j, \frac{2\pi}{\omega_0}\Big) &= \deg_B\Big(\mathcal{H}^-\Big(v^*, \tau_j, \frac{2\pi}{\omega_0}\Big), \Omega_{\xi, \frac{2\pi}{\omega_0}}\Big) - \deg_B\Big(\mathcal{H}^+\Big(v^*, \tau_j, \frac{2\pi}{\omega_0}\Big), \Omega_{\xi, \frac{2\pi}{\omega_0}}\Big) \\ &= -1. \end{aligned}$$

Consequently, we have

$$\sum_{\left(v^*,\tau_j,2\pi/\omega_0\right)\in D(v^*,\tau,s)\cap N(F)} \gamma(v^*,\tau,s) < 0, \tag{3.5}$$

Besides, $D(v^*,\tau,s)$ is nonempty.

From the theorem 3.3 in [28], it follows that $D\left(v^*,\tau_j,\frac{2\pi}{\omega_0}\right)$ is unbounded. The proof is completed. □

Lemma 3.2 *All the periodic solutions of system (2.3) are uniformly bounded in* $\mathbb{R}^2_+$.

Proof Let $(x(t),N(t))$ be a nonconstant periodic solution of system(2.3) in $\mathbb{R}^2_+$. Set

$$\begin{aligned} M_1 &= \max\{x(t)|t\geq 0\} = x(\eta_1), \qquad & M_2 &= \max\{N(t)|t\geq 0\} = N(\eta_2),\\ m_1 &= \min\{x(t)|t\geq 0\} = x(\xi_1), \qquad & m_2 &= \min\{N(t)|t\geq 0\} = N(\xi_2). \end{aligned}$$

Due to the assumption that $N(t)\geq 0$ for all $t\geq 0$, we have

$$\begin{aligned} 0 &= r(1-M_1^3) - \frac{kN(\eta_1)}{1+N(\eta_1)} \leq r(1-M_1^3),\\ 0 &= r(1-m_1^3) - \frac{kN(\xi_1)}{1+N(\xi_1)} \geq r(1-m_1^3) - k. \end{aligned}$$

Then, it's easy to obtain

$$\max\left\{0,\left(1-\frac{k}{r}\right)^{1/3}\right\} \leq m_1 \leq M_1 \leq 1, \tag{3.6}$$

Meanwhile, we note that

$$\begin{aligned} 0 &= \rho x^2(\eta_2-\tau)N(\eta_2-\tau) - dM_2^2 \leq \rho M_1^2 N(\eta_2-\tau) - dM_2^2,\\ 0 &= \rho x^2(\xi_2-\tau)N(\xi_2-\tau) - dm_2^2 \geq \rho m_1^2 N(\xi_2-\tau) - dm_2^2. \end{aligned}$$

A direct calculation yields

$$\frac{\rho m_1^2}{d} \leq m_2 \leq M_2 \leq \frac{\rho M_1^2}{d}. \tag{3.7}$$

This shows the periodic solutions of system (2.3) in the first quadrant is uniformly bounded. The proof is completed. □

We comment that the bounded solutions to system (2.3) represents the tumor mass cannot grow unrestrictedly. This means that we may control the tumor volume.

Lemma 3.3 *The system (2.3) has no* $\tau-$ periodic solution *under the assumption*

$$(H_2)\quad \rho \leq 3r.$$

Proof Let $(x(t),N(t))$ be a periodic solution to (2.3) with period τ. Then it also is a periodic solution for the following ODE system

$$\begin{cases} \dot{x}(t) = r[1-x^3(t)] - \dfrac{kN(t)}{1+N(t)},\\ \dot{N}(t) = \rho x^2(t)N(t) - dN^2(t). \end{cases} \tag{3.8}$$

Let $(f(x,N),g(x,N))$ be the vector filed of (3.8), then for all $(x,N)\in\mathbb{R}^2_+$, we have

$$\frac{\partial f}{\partial x} + \frac{\partial g}{\partial N} = (\rho-3r)x^2 - 2dN. \tag{3.9}$$

Under the condition (H_2), we have $\frac{\partial f}{\partial x} + \frac{\partial g}{\partial N} < 0$. By the classical Bendixson's negative criterion [32], it can be claimed that the system (3.8) has no nonconstant periodic solutions lying entirely in the first quadrant. □

Proposition 1 *Suppose* (H_2) *is true, then system (2.3) has no periodic solutions.*

Theorem 3.1 *Suppose that all solutions of system (2.3) are nonnegative,* (H_1) *and* (H_2) *hold, then system (2.3) has at least* j *positively periodic solutions when* $\tau>\tau_j$, $j=1,2,\ldots$ *with* τ_j *defined in (2.13).*

Proof According to the discussion in the beginning of this section, we know that $\left(v^*, \tau_j, \frac{2\pi}{\omega_0}\right)$ is isolate centers. Then $D\left(v^*, \tau_j, \frac{2\pi}{\omega_0}\right)$ is unbounded following Lemma 3.1. Meanwhile, Lemma 3.2 suggests that the projection of $D\left(v^*, \tau_j, \frac{2\pi}{\omega_0}\right)$ onto $v-$space is bounded. From Proposition 1, one knows the projection of $D\left(v^*, \tau_j, \frac{2\pi}{\omega_0}\right)$ onto $\tau-$space is bounded below.

By the definition of τ_j in (2.13), one know that $2\pi < \tau_j\omega_0 < (2j+1)\pi$ for $j \geq 1$, then

$$\frac{\tau_j}{j+1} < \frac{2\pi}{\omega_0} < \tau_j. \tag{3.10}$$

Employing Lemma 3.3, it is clear that if $(v, \tau, s) \in D\left(v^*, \tau_j, \frac{2\pi}{\omega_0}\right)$, then $\frac{\tau}{j+1} < s < \tau$. This implies that the projection of $D\left(v^*, \tau_j, \frac{2\pi}{\omega_0}\right)$ onto the $\tau-$space has to be unbounded so that $D\left(v^*, \tau_j, \frac{2\pi}{\omega_0}\right)$ can be unbounded. As a result, the projection of $D\left(v^*, \tau_j, \frac{2\pi}{\omega_0}\right)$ onto the $\tau-$space covers $[\tau_j, \infty)$. Thus, for each $\tau > \tau_j$, system (2.3) has j nonconstant periodic solutions. Based on Lemma 3.2, one can get the positivity of these periodic solutions. The proof is completed. □

Remark 3.1 *Since $0 < \omega_0\tau_0 < 2\pi$, we have $\tau_0 < \frac{2\pi}{\omega_0} < \infty$. It has been known that the projection of $D\left(v^*, \tau_j, \frac{2\pi}{\omega_0}\right)$ onto the $v-$space is bounded. Thus, for $(v, \tau, s) \in D\left(v^*, \tau_j, \frac{2\pi}{\omega_0}\right)$, the unboundedness of $D\left(v^*, \tau_j, \frac{2\pi}{\omega_0}\right)$ yields that the projection of $D\left(v^*, \tau_j, \frac{2\pi}{\omega_0}\right)$ onto the $s-$space or $\tau-$space may be unbounded. This indicates that the projection of $D\left(v^*, \tau_j, \frac{2\pi}{\omega_0}\right)$ onto the $\tau-$space may not cover $[\tau_0, \infty)$. If we can further verify that the periods of periodic solutions bifurcating from (E_*, τ_0) is bounded, then under conditions (H_1) and (H_2), system (2.3) has at least $j+1$ positively periodic solutions for $\tau > \tau_j$, $j = 0, 1, 2, \ldots$.*

4. Numerical simulations

In this section, some numerical simulations are conducted to support the previous theoretical analysis. In particular, we numerically study the ratio of the immune killing rate to tumor volume growth rate, behaviors of Hopf bifurcations, and functional relations between the first bifurcation value of the immune response time and other parameters. Considering Table 1.1, we choose the following parameter values:

$$T_m = 0.5,\ r = 0.29,\ k = 0.9,\ d = 0.5\ ,\ \rho = 0.24,\ \beta = 0.11$$

4.1. The effect of the killing rate and growth rate

We show the stability change of positive equilibrium driven by the ratio $\frac{k}{r}$. In Figure 2(a), the black line is denoted by $P(r,k) = 9rx_* - \frac{2k\rho}{d(1+N_*)^2}$ and the red line stands for $k = r$. It can be checked that the points satisfying $B < D$ are in the part above the black line. The region under the red line holds $k < r$ and $B > D$, which indicates that the coexisting state of tumor and CTLs is stable when the growth rate of tumor is greater than the killing rate of CTLs. As the ratio increases and crosses the black line, the result in Theorem 2.5 shows the stability of positive equilibrium switches and a family of periodic solutions appear. In addition, oscillations of immune cell number have been observed in some clinical contexts, for example [6]. It is clear that there is a critical value of the ratio, below which the positive equilibrium is locally asymptotically stable and above which periodic solutions appear. Understanding how the CTLs recruitment and death rate affect $\frac{k}{r}$ inspires our interest since the

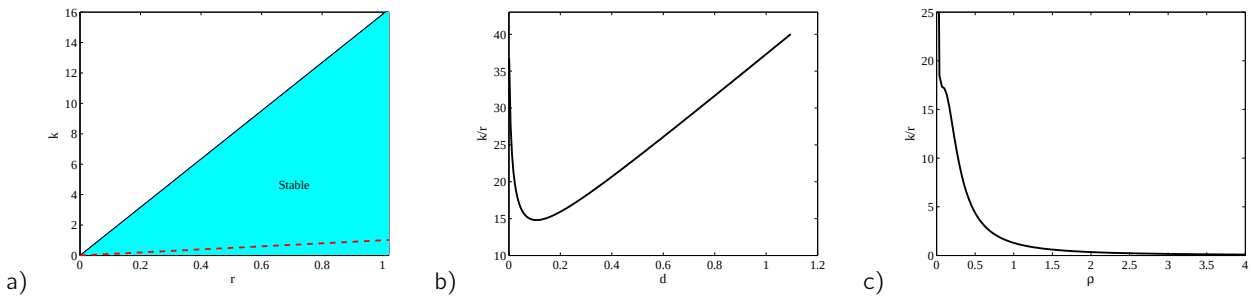

Figure 2. (a):the black and red lines are determined by $P(r,k) = 9rx_* - \frac{2k\rho}{d(1+N_*)^2} = 0$ and $k = r$, respectively. $P(r,k) < 0$ above the black line and $P(r,k) > 0$ below the black line; (b): the effect of d on $\frac{k}{r}$; (c): the effect of ρ on $\frac{k}{r}$.

ratio determines the competition outcome between CTLs and tumor cells. As illustrated in Figure 2(c), CTLs recruitment has a negative effect on the ratio. While the ratio first rapidly decreases then gradually increases as CTLs death speed goes up, as shown in 2(b). We also know that it is more possible for the system (2.3) to undergoes the Hopf bifurcation with a large value

of $\frac{k}{r}$. Therefore, when more CTLs die or less CTLs are activated, the stable coexistence of tumor and CTLs will be broken and the volume of the tumor changes in period.

In view of the first equation of system (1.2), we find $0 \leq T(t) \leq T_m$. This means a solid tumor cannot grow infinitely. It is known that the size of a tumor indicates the grade malignancy of a tumor, if the tumor volume reaches certain size, the patient will die. In this study, we have found that the tumor volume may change periodically when the immune response time is long. Once the volume is greater than a specific value, the patient can not be cured and such oscillations disappear. Suppose that the critical value is $T_0 = 3 \times 10^6 \mu m^3$. Define *survival time* by the first time that the tumor size reaches to T_0. We numerically explore the effect of immune delay on the survival time, which is shown in Figure 3. It is clear that shorter response time of the adaptive immune system leads to longer survival time for the patient. Further, the survival time will not decrease to zero and it has a minimum value, which is reasonable clinically.

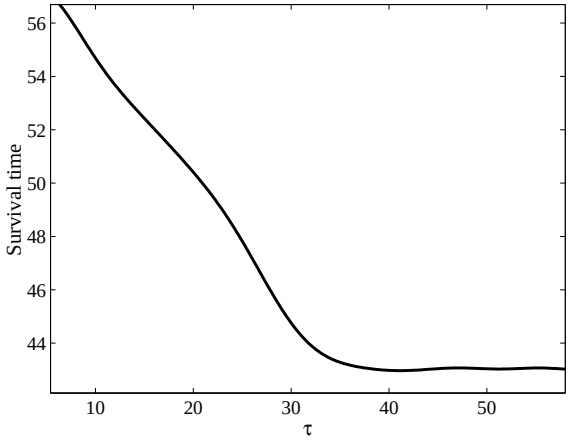

Figure 3. Survival time varies with immune delay when initial values are $T(t) = 0.01, N(t) = 0.82$.

4.2. Numerical simulations of Hopf bifurcation

With the same group of parameter values, some calculations show that the unique positive equilibrium is $(0.3968, 0.4238)$ and the condition $B < D$ is satisfied. Furthermore, we obtain the first Hopf bifurcation value $\tau_0 \approx 13.4$, and $\omega_0 \approx 0.07$. Applying Theorem 2.3, E_* is locally asymptotically stable when $\tau \in [0, \tau_0)$. When τ passes through τ_0, E_* loses its stability and a family of periodic solutions appear if $\tau > \tau_0$.

Next, we consider the properties of Hopf bifurcations at the first Hopf bifurcation value. It can be calculated that: $g_{02} \approx -50.1279 - 15.5860i$, $g_{20} \approx -50.1279 + 15.5860i$, $g_{11} \approx 47.2462 - 10.7824i$, $g_{21} \approx -2291.2983 - 7694.8892i$. Moreover, we obtain $c_1(0) \approx -1779.8039 - 7729.1143$. Thus, $\mu_2 \approx 7.7066$, $\beta_2 \approx -3559.6078$, $T_2 \approx 7537.1536$. Obviously, $\mu_2 > 0$, $\beta_2 < 0$ and $T_2 > 0$, which imply that Hopf bifurcation is forward; the periodic solutions are asymptotically stable and their periods increase with time delay. The above results are illustrated in Figure 4 and Figure 5.

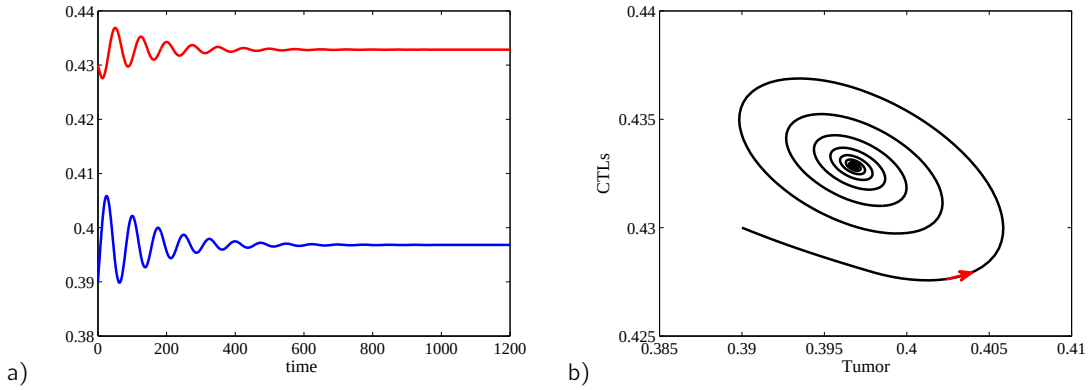

Figure 4. The positive equilibrium of system (2.3) is locally asymptotically stable when $\tau = 9 \in [0, \tau_0)$. (The red curve represents CTL cells and the blue one is about tumor cells.)

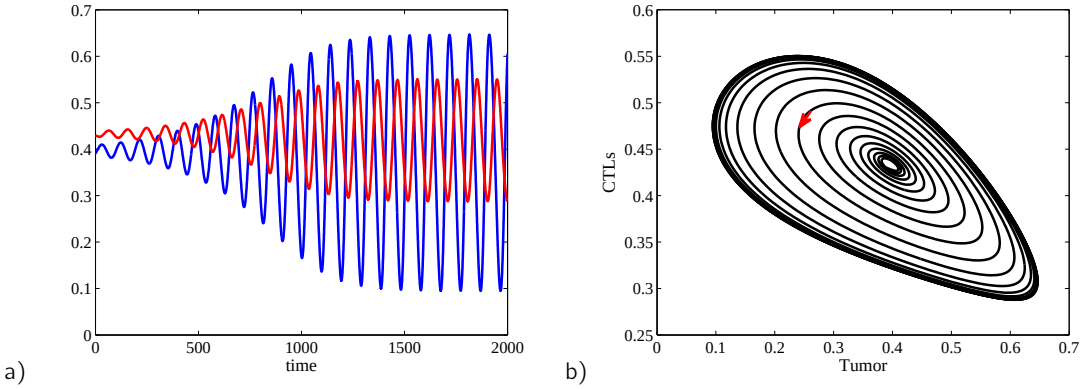

Figure 5. When $\tau = 17 > \tau_0$, there is a stable periodic solution bifurcating from the positive equilibrium. (The red curve represents CTL cells and the blue one is about tumor cells.)

With the same parameters, we simulate the global behavior of solutions. The Hopf bifurcation diagrams are shown in Figure 6. We see that there is a global continuation of periodic solution bifurcating from Hopf bifurcation when $\tau > \tau_j$, $j \geq 1$. Besides, the amplitude of the periodic solution raises with the parameter τ increasing.

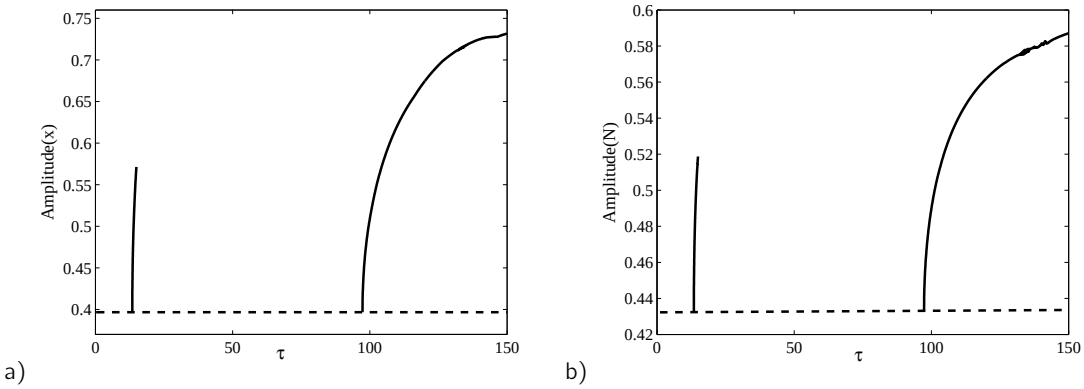

Figure 6. The amplitudes of the first two branches of periodic solutions with the initial value $(0.3968, 0.4328)$.

4.3. Numerical simulations concerning other parameters

The earlier a tumor is detected, the easier it is cleared out. In this subsection, we numerically explore how other factors in the system (2.3) affect the adaptive immune response time, namely the first bifurcation value τ_0.

It is natural that the amount of CTLs has relations with τ_0. Assume that all other parameters remain fixed, then we find that the first bifurcation value τ_0 increases with the CTLs death rate, see Figure 7(a), which suggests that the immune response time increases when more CTLs cells die. In this case, we may claim that the tumor and immune cells easily attain a periodical interacting fashion. Furthermore, we find that the immune response time becomes smaller as the recruitment rate increases, as shown in Figure 7(b). This is easy to understand. In fact the larger recruitment rate means more immune cells are recruited to the cancer site, which is beneficial to the coexistence of tumor and CTLs cells.

The paper [10] and the assumption (H_1) in this paper both point out that the ratio $\frac{k}{r}$ mostly reflects on the tumor-CTLs interaction dynamics. When other parameters remain unaltered, it can be found that the value of τ_0 is large if tumor growth is fast, which is shown in Figure 8(a). In Figure 8(b), we can see the change of τ_0 is affected by the tumor growth together with CTLs killing action. The joint effect of growth rate and killing rate is presented in Figure (9).

5. Conclusion

In this work, a two-dimensional tumor-immune model with the time delay of the adaptive immune response is studied from the point of view of bifurcation analysis. The avascular growth of a spherical solid tumor is achieved by the proliferating layer cells which is restricted by nutrient supply, thus the tumor has a finite final size. However, we find both zero and maximum tumor volume equilibria are unstable. Inspired by the fact that dead cells form the necrotic core inside the tumor, we propose the surface

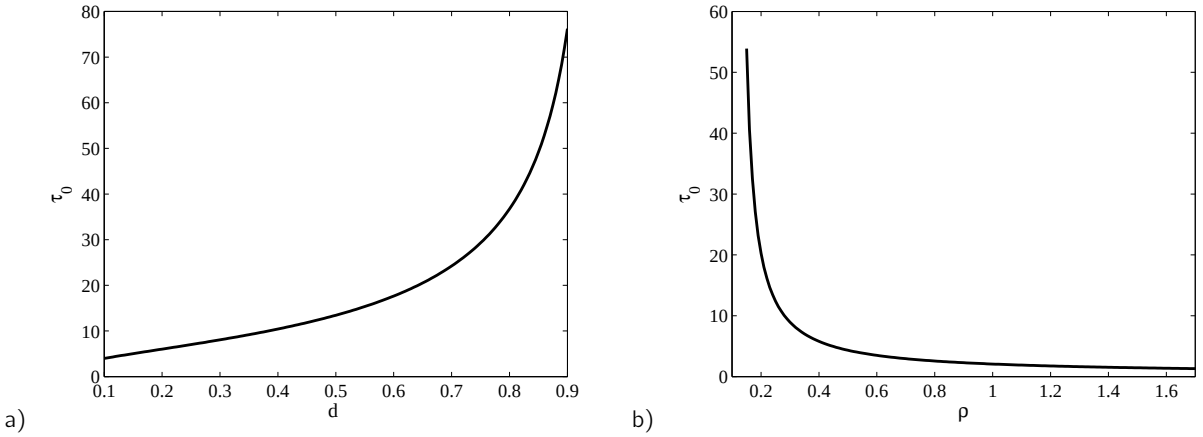

Figure 7. (a): The variation of τ_0 with CTL death rate d. (b): The variation of τ_0 with CTL recruitment rate ρ.

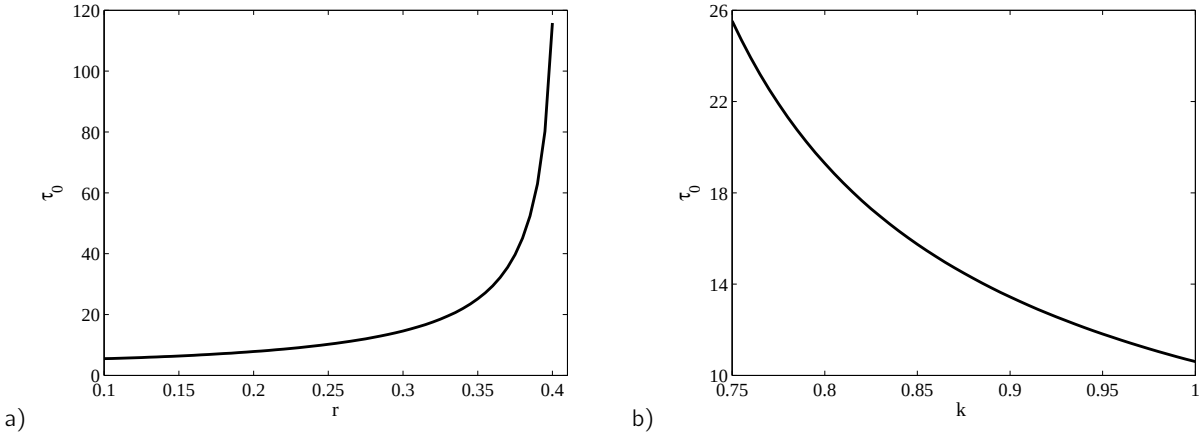

Figure 8. (a): Numerical simulation of τ_0 for varying growth rate r. (b): Numerical simulation of τ_0 for varing killing rate k.

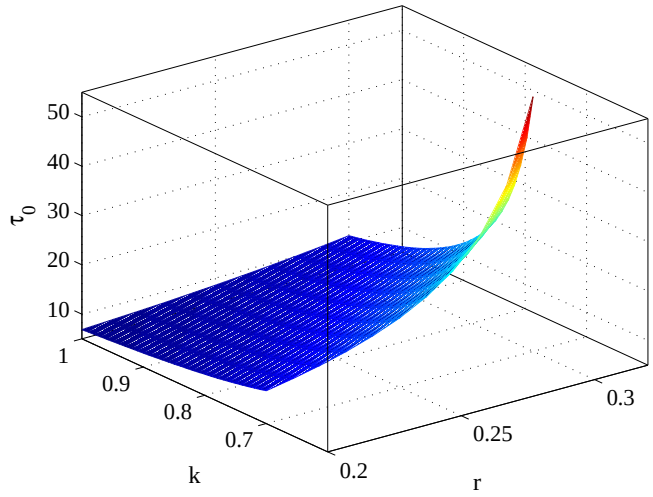

Figure 9. Numerical simulation of τ_0 affected by k and r together.

growth idea. If the immune system can recognize and attack the tumor in this phase, then it's possible to control the growth of a tumor. We assume the immune response only occurs on the surface of a tumor, so the response function includes the tumor

surface area.

For model (2.3), we confirm that there is a unique coexistent equilibrium and its dynamical behavior is roughly determined by the ratio of the immune killing rate to tumor volume growth rate. The positive equilibrium is locally asymptotically stable when the ratio is smaller than a critical value, and unstable otherwise. The adaptive immune response time delay significantly impacts the stability of the positive equilibrium, which drives the system to undergo Hopf bifurcations under certain conditions. We obtain explicit formulas to determine bifurcation direction and stability of bifurcating periodical solutions. We show the global existence of Hopf bifurcation.

Numerically, we find that a shorter immune response time leads to a longer patient survival time and the period and amplitude of a stable periodic solution increase with the immune response time. When CTLs recruitment rate and death rate vary, we observe how the ratio of the immune killing rate to tumor volume growth rate and the first bifurcation value of the immune response time change numerically, which yields further insights to the tumor-immune dynamics.

It is known that the innate immune system serves as a first defense line. The innate immune system may have different effect on tumor growth [33]. We only consider the adaptive immune response mediated by CTLs in this work. It is necessary to incorporate the innate immune response into modeling of tumor-immune interaction in order to achieve a complete understanding. We plan to consider both innate immune response and adaptive immune response in our future study.

Acknowledgements

The authors would like to express their thanks to the referees for their valuable suggestions. HZ, BN and YXG acknowledge the supports from National Natural Science Foundation of China (11701120), Shandong Provincial Natural Science Foundation (ZR2019Q020) and the Innovation Foundation at HIT(WH). JPT acknowledges the supports from National Institutes of Health (U54CA132383), National Science Foundation of US (DMS-1446139) and National Natural Science Foundation of China (No.11371048).

Conflict of interests

The authors declare that they have no conflict of interest.

Appendix

In this section, we choose τ as a bifurcating parameter and derive the explicit formulas determining the properties of Hopf bifurcation under the assumption (H_1). The techniques to be used are normal form method and the centre manifold theory presented in [25, 26].

Without loss of generality, write $\tau = \tilde{\tau} + \mu$, then $\mu = 0$ is a Hopf bifurcation point for system (2.3). Let $x_1(t) = x(t\tau) - x_*$, $x_2(t) = N(t\tau) - N_*$, system (2.3) becomes

$$\begin{cases} \dot{x}_1(t) = (\tilde{\tau}+\mu)\left[r(1-(x_1(t)+x_*)^3) - \dfrac{k(x_2(t)+N_*)}{1+x_2(t)+N_*}\right], \\ \dot{x}_2(t) = (\tilde{\tau}+\mu)\left[\rho(x_1(t-1)+x_*)^2(x_2(t-1)+N_*) - d(x_2(t)+N_*)^2\right]. \end{cases} \tag{5.1}$$

For $\varphi = (\varphi_1, \varphi_2)^T \in C([-1,0],\ \mathbb{R}^2)$, let

$$L_\mu\varphi = (\tilde{\tau}+\mu)B_1\varphi(0) + (\tilde{\tau}+\mu)B_2\varphi(-1),$$

with $B_1 = \begin{pmatrix} -3rx_*^2 & \frac{-k}{(1+N_*)^2} \\ 0 & -2dN_* \end{pmatrix}$, $B_2 = \begin{pmatrix} 0 & 0 \\ -2\rho x_* N_* & -\rho x_*^2 \end{pmatrix}$. And

$$f(\mu,\varphi) = (\tilde{\tau}+\mu)\begin{pmatrix} \frac{k\varphi_2^2(0)}{(1+N_*)^3} - \frac{k\varphi_2^3(0)}{(1+N_*)^4} - 3rx_*\varphi_1^2(0) - r\varphi_1^3(0) + O(4) \\ \rho\varphi_1^2(-1)\varphi_2(-1) + \rho N_*\varphi_1^2(-1) - d\varphi_2^2(0) + 2\rho x_*\varphi_1(-1)\varphi_2(-1) \end{pmatrix}. \tag{5.2}$$

By the Riesz representation theorem, there is a function $\eta(\cdot,\mu) : [-1,0] \to \mathbb{R}^2$ of bounded variation, such that

$$L_\mu\varphi = \int_{-1}^{0} d\eta(\theta,\mu)\varphi(\theta), \quad for\ \varphi \in C([-1,0],\ \mathbb{R}^2).$$

In fact, $\eta(\cdot,\mu)$ can be taken as

$$\eta(\mu,\theta) = \begin{cases} (\tilde{\tau}+\mu)B_1, & \theta = 0, \\ 0 & \theta \in (-1,0), \\ (\tilde{\tau}+\mu)B_2, & \theta = -1, \end{cases}$$

For $\varphi \in C^1([-1,0],\mathbb{R}^2)$, define

$$A(\mu)\varphi(\theta)=\begin{cases}\frac{\mathrm{d}\varphi(\theta)}{\mathrm{d}\theta}, & \theta\in[-1,0),\\ \int_{-1}^{0}\mathrm{d}\eta(\mu,\theta)\varphi(\theta), & \theta=0,\end{cases},\quad R(\mu)\varphi(\theta)=\begin{cases}0, & \theta\in[-1,0),\\ f(\mu,\varphi), & \theta=0.\end{cases}$$

Then, system (2.3) is equivalent to the following abstract form

$$\dot{x}_t=A(\mu)x_t+R(\mu)x_t. \tag{5.3}$$

with $x=(x_1,x_2)^T$, $x_t(\theta)=x(t+\theta)$, $\theta\in[-1,0]$. For $\psi\in C^1([0,1],\ \mathbb{R}^2)$, denote the adjoint operator of $A(\mu)$ by

$$A^*(\mu)\psi(s)=\begin{cases}-\dfrac{\mathrm{d}\psi(s)}{\mathrm{d}s}, & s\in(0,1],\\ \displaystyle\int_{-1}^{0}\psi(-t)\mathrm{d}\eta(t,s), & s=0.\end{cases}$$

The discussion at the beginning of section 2 implies that $\pm i\tilde{\tau}\omega_0$ are eigenvalues of $A(0)$ and they are also eigenvalues of $A^*(0)$. Let $q(\theta)=(1,\ P)^T e^{i\omega_0\tilde{\tau}\theta}$, $q^*(s)=E(Q,\ 1)e^{-i\omega_0\tilde{\tau}s}$ be the corresponding eigenvectors of $A(0)$ and $A^*(0)$, respectively. Then, using the following bilinear form

$$\langle\psi,\varphi\rangle=\bar{\psi}(0)\varphi(0)-\int_{-1}^{0}\int_{\xi=0}^{\theta}\bar{\psi}(\xi-\theta)\mathrm{d}\eta(\theta)\varphi(\xi)\mathrm{d}\xi,$$

with $\varphi\in C^1([-1,0],\mathbb{R}^2)$, $\psi\in C^1([1,0],\mathbb{R}^2)$ and $\eta(\theta)=\eta(\theta,0)$, we have

$$P=-\frac{(3rx_*^2+i\omega_0)(1+N_*)^2}{k},\quad Q=\frac{(i\omega_0-2dN_*+\rho x_*^2e^{i\omega_0\tilde{\tau}})(1+N_*)^2}{k}.$$
$$E=\left[(Q+\bar{P})+e^{i\omega_0\tilde{\tau}}\tilde{\tau}(2\rho x_*N_*+\rho x_*^2\bar{P})\right]^{-1}.$$

In what follows, we applying the notations in [25]. Based on the center manifold theorem, we set $W(t,\theta)=W(z(t),\bar{z}(t),\theta)$ on the center manifold $\mathcal{C}_0$ with

$$W(z,\bar{z},\theta)=W_{20}(\theta)\frac{z^2}{2}+W_{11}(\theta)z\bar{z}+W_{02}(\theta)\frac{\bar{z}^2}{2}+W_{30}(\theta)\frac{z^3}{6}+\ldots,$$

The solution x_t of system (5.1) at $\mu=0$ can be written as

$$x_t=2\mathrm{Re}(z(t)q)+W(z(t),\bar{z}(t))$$

where $z(t)=\langle q*,x_t\rangle$. We further have

$$\begin{aligned}\dot{z}(t)&=i\omega_0\tilde{\tau}z+\bar{q}^*(\theta)f(0,w(z,\bar{z},\theta)+2\mathrm{Re}(zq(\theta)))\\&=i\omega_0\tilde{\tau}z+\bar{q}^*(0)f(0,w(z,\bar{z},0)+2\mathrm{Re}(zq(0)))\\&=i\omega_0\tilde{\tau}z+\bar{q}^*(0)f_0.\end{aligned}\tag{5.4}$$

Rewrite it as

$$\dot{z}(t)=i\omega_0\tilde{\tau}z(t)+g(z,\bar{z}),\tag{5.5}$$

where

$$g(z,\bar{z})=g_{20}\frac{z^2}{2}+g_{11}z\bar{z}+g_{02}\frac{z^2}{2}+g_{21}\frac{z^2\bar{z}}{2}+\cdots.$$

Therefore,

$$\begin{aligned}g_{20}&=2\bar{E}\tilde{\tau}(\bar{Q},1)\begin{pmatrix}\frac{kP^2}{(1+N_*)^3}-3rx_*\\ \rho N_*e^{-2i\omega_0\tilde{\tau}}-dP^2+2\rho x_*Pe^{-2i\omega_0\tilde{\tau}}\end{pmatrix},\\ g_{11}&=\bar{E}\tilde{\tau}(\bar{Q},1)\begin{pmatrix}\frac{2kP\bar{P}}{(1+N_*)^3}-6rx_*\\ 2\rho N_*-2dP\bar{P}+2\rho x_*(P+\bar{P})\end{pmatrix},\\ g_{21}&=2\bar{E}\tilde{\tau}(\bar{Q},1)\begin{pmatrix}m_{11}+m_{12}+m_{13}\\ m_{21}+m_{22}+m_{23}+m_{24}\end{pmatrix},\end{aligned}\tag{5.6}$$

where

$$m_{11}=\frac{k}{(1+N_*)^3}\Big[W_{20}^{(2)}(0)\bar{P}+2W_{11}^{(2)}(0)P\Big],\quad m_{12}=-3rx_*\Big[W_{20}^{(1)}(0)+2W_{11}^{(1)}(0)\Big],$$
$$m_{13}=-\frac{3kP\bar{P}}{(1+N_*)^4}-3r,\quad m_{22}=\rho N_*\Big[W_{20}^{(1)}(-1)e^{i\omega_0\tilde{\tau}}+2W_{11}^{(1)}(-1)e^{-i\omega_0\tilde{\tau}}\Big],$$
$$m_{21}=2\rho x_*\Big[e^{i\omega_0\tilde{\tau}}\big(W_{20}^{(1)}(-1)\bar{P}+W_{20}^{(2)}(-1)\big)+e^{-i\omega_0\tilde{\tau}}\big(W_{11}^{(1)}(-1)P+W_{11}^{(2)}(-1)\big)\Big],$$
$$m_{23}=-d\Big[W_{20}^{(2)}(0)\bar{P}+2W_{11}^{(2)}(0)P\Big],\quad m_{24}=\rho(2P+\bar{P})e^{-i\omega_0\tilde{\tau}}.$$

Note that the value of g_{21} depends on $W_{20}(\theta)$ and $W_{11}(\theta)$, hence, we need also to compute $W_{20}(\theta)$ and $W_{11}(\theta)$. In view of (5), it follows that

$$\begin{aligned}\dot{W}&=\dot{x}_t-\dot{z}q-\dot{\bar{z}}\bar{q}=\begin{cases}A(0)W-2Re(\bar{q}^*(0)f_0q(\theta)),\ \theta\in[-1,0),\\ A(0)W-2Re(\bar{q}^*(0)f_0q(0))+f_0,\ \theta=0\end{cases}\\&\overset{\text{def}}{=}A(0)W+H_{20}(\theta)\frac{z^2}{2}+H_{11}(\theta)z\bar{z}+H_{02}(\theta)\frac{\bar{z}^2}{2}+\dots\end{aligned}\tag{5.7}$$

Due to the chain rule

$$\dot{W}=\frac{\partial W(z,\bar{z})}{\partial z}\dot{z}+\frac{\partial W(z,\bar{z})}{\partial\bar{z}}\dot{\bar{z}},$$

then

$$(A(0)-2i\omega_0\tilde{\tau})W_{20}(\theta)=-H_{20}(\theta),\quad A(0)W_{11}(\theta)=-H_{11}(\theta).\tag{5.8}$$

Note that for $\theta\in[-1,0)$,

$$\begin{aligned}H(z,\bar{z},\theta)&=-q^*(0)f_0q(\theta)-q^*(0)\bar{f}_0\bar{q}(\theta)\\&=-g(z,\bar{z})q(\theta)-\bar{g}(z,\bar{z})\bar{q}(\theta),\end{aligned}$$

this leads to

$$H_{20}(\theta)=-g_{20}q(\theta)-\bar{g}_{02}\bar{q}(\theta),\quad H_{11}(\theta)=-g_{11}q(\theta)-\bar{g}_{11}\bar{q}(\theta),\ \theta\in[-1,0).\tag{5.9}$$

From (5.8), we have

$$\begin{aligned}W_{20}(\theta)&=\frac{ig_{20}}{\omega_0\tilde{\tau}}q(0)e^{i\omega_0\tilde{\tau}\theta}+\frac{i\bar{g}_{02}}{3\omega_0\tilde{\tau}}q(0)e^{-i\omega_0\tilde{\tau}\theta}+M_1e^{2i\omega_0\tilde{\tau}\theta},\\W_{11}(\theta)&=-\frac{ig_{11}}{\omega_0\tilde{\tau}}q(0)e^{i\omega_0\tilde{\tau}\theta}+\frac{i\bar{g}_{11}}{\omega_0\tilde{\tau}}\bar{q}(0)e^{-i\omega_0\tilde{\tau}\theta}+M_2,\end{aligned}\tag{5.10}$$

where M_1 and M_2 are both 2-dimension vectors.

As $\theta=0$ in (5.7) and (5.8), together with the definition of A, we have

$$\begin{aligned}H_{20}(0)&=-g_{20}q(0)-\bar{g}_{02}\bar{q}(0)+\begin{pmatrix}\frac{2kP^2}{(1+N_*)^3}-6rx_*\\2\rho N_*e^{-2i\omega_0\tilde{\tau}}-2dP^2+4\rho x_*Pe^{-2i\omega_0\tilde{\tau}}\end{pmatrix},\\H_{11}(0)&=-g_{11}q(0)-\bar{g}_{11}\bar{q}(0)+\begin{pmatrix}\frac{2kP\bar{P}}{(1+N_*)^3}-6rx_*\\2\rho N_*-2dP\bar{P}+2\rho x_*(P+\bar{P})\end{pmatrix}.\end{aligned}\tag{5.11}$$

It follows that

$$\begin{pmatrix}2i\omega_0+3rx_*^2 & \frac{k}{(1+N_*)^2}\\-2\rho x_*N_*e^{-2i\omega_0\tilde{\tau}} & 2i\omega_0-\rho x_*^2e^{-2i\omega_0\tilde{\tau}}+2dN_*\end{pmatrix}M_1=\begin{pmatrix}\frac{2kP^2}{(1+N_*)^3}-6rx_*\\2\rho N_*e^{-2i\omega_0\tilde{\tau}}-2dP^2+4\rho x_*Pe^{-2i\omega_0\tilde{\tau}}\end{pmatrix}.\tag{5.12}$$

and

$$\begin{pmatrix}3rx_*^2 & \frac{k}{(1+N_*)^2}\\-2\rho x_*N_* & -\rho x_*^2+2dN_*\end{pmatrix}M_2=\begin{pmatrix}\frac{2kP\bar{P}}{(1+N_*)^3}-6rx_*\\2\rho N_*-2dP\bar{P}+2\rho x_*(P+\bar{P})\end{pmatrix}\tag{5.13}$$

Now $W_{20}(\theta)$ and $W_{11}(\theta)$ could be obtained and g_{21} could be presented explicitly. Consequently, $c_1(0)$ and other quantities could be directly expressed in terms of parameters and delay mentioned in (5.1).

$$\begin{aligned}c_1(0)&=\frac{i}{2\omega_0\tilde{\tau}}\Big(g_{11}g_{20}-2\mid g_{11}\mid^2-\frac{\mid\bar{g}_{20}\mid^2}{3}\Big)+\frac{g_{21}}{2},\\\mu_2&=-\frac{\mathrm{Re}(c_1(0))}{\mathrm{Re}(\lambda_0'(\tilde{\tau}))},\\\beta_2&=2\mathrm{Re}(c_1(0)),\\T_2&=-\frac{\mathrm{Im}(c_1(0))+\mu_2\mathrm{Im}(\lambda_0'(\tilde{\tau}))}{\omega_0}.\end{aligned}\tag{5.14}$$

According to the general Hopf bifurcation theory (see [25]), it is known that μ_2 determines the direction of Hopf bifurcation: if $\mu_2>0$ ($\mu_2<0$), then a branch of periodic solutions appear for $\tau>\tilde{\tau}$ ($\tau<\tilde{\tau}$); β_2 determines the stability of the bifurcating periodic solutions: the bifurcating periodic solutions in the center manifold are stable (unstable) if $\beta_2<0$ ($\beta_2>0$); T_2 determines the period: the period increases (decreases) if $T_2>0$ ($T_2<0$).

References

1. Wang W, Epler JE, Salazar LG, Riddell SR. Recognition of braest cancer cells by $CD8_+$ cytotoxic T-cell clones specific for NY-BR-1. *Cancer Res*. 2006; 66:6826-6833.
2. Kaufman HL, Kohlhapp FJ, Zloza A. Oncolytic viruses: a new class of immunotherapy drugs. *Nature Reviews Drug Discovery*. 2015; 14:642-662.
3. Byrne HM, Alarcon A, Owen MR, Webb SD, Maini P. Modeling aspects of cancer dynamics: a review. *Philos. Trans. R. Soc. Lons. Ser. A Math. Phys. Eng. Sci*. 2006; 364:1563-1578.
4. Li F, Ma W. Dynamics analysis of an HTLV-1 infection model with mitotic division of actively infected cells and delayed CTL immune response. *Math. Meth. Appl. Sci*. 2018;1-18.
5. Nagy JD. The ecology and evolutionary biology of cancer: a review of mathematical model of necrosis and tumour cell diversity. *Math. Biosci. Eng*. 2017; 2:381-418.
6. D′Onofrio A. A general framework for modeling tumor-immune system competition and immunotherapy: mathematical analysis and biomedical inferences. *Phys. D*. 2005; 208:220-235.
7. Adam JA, Bellomo N. *A survey of models for tumor-immune system dynamics*, Birkhäuser Boston,1997.
8. Eftimie R, Bramson JL, Earn DJD. Interaction between the immune system and cancer: a brief review of non-spatial mathematical models. *Bull. Math. Biol*. 2011; 73:2-32.
9. Kuznetsov VA, Makalkin IA, Taylor MA, Perelson A. Nonlinear dynamics of immunogenic tumors: parameter estimation and global bifurcation analysis. *Bull. Math. Biol*. 1994; 56:295-312.
10. Frascoli F, Kim PS, Hughes BD, Landman KA. A dynamical model of tumour immunotherapy. *Math. Biosci*. 2014; 253:50-62.
11. Nestle FO, Tonel G, Farkas A. Cancer vaccines: the next generation of tools to monitor the anticancer immune response. *PLoS Medici*. 2005; 2:em339.
12. Kansal AR, Torquato S, GR IVH, Chiocca E. Simulated brian tumor growth dynamics using a three-dimensional cellular automaton. *J. Theoret. Biol*. 2000; 203:367-382.
13. Liu Y, Zeng G. Caner and innate immune system interactions: translational potentials for cancer immunotherapy. *J. Immunother*. 2012; 35:299-308.
14. Dranoff G. (2004) Cytokines in cancer pathogenesis and cancer therapy. *Nature Review Cancer*. 2004; 4:11-22.
15. Bi P, Ruan S, Zhang X. Periodic and chaotic oscillations in a tumor and immune system interaction model with three delays. *Chaos*. 2014; 24:288-299.
16. Villasana M, Radunskaya A. A delay differential equation model for tumor growth. *J. Math. Biol*. 2003; 47:270-294.
17. Liu Y, Wei J. Dynamical analysis in a diffusive predator-prey system with a delay and strong Allee effect. *Math. Meth. Appl. Sci*. 2019;1-18.
18. Kaslik E, Neamtu M. Stability and Hopf bifurcation analysis for the hypothalamic-pituitary-adrenal axis model with memory. *Math. Med. Biol*. 2018; 35:49-78.
19. Barza PA. Predator-prey dynamics with square root functional responses. *Nonlinear Anal. Real World Appl*. 2012; 13:1837-1843.
20. Chattopadhyay J, Chatterjee S, Venturino E. Patchy agglomeration as a transition from monospecies to recurrent plankton blooms. *J. Theoret. Biol*. 2008; 253:289-295.
21. Friedman A, Tian JJP, Fulci G, Chiocca EA, Wang J. Glioma virotherapy: the effects of innate immune suppression and increased viral replication capacity. *Cancer Res*. 2006; 66:2314-2319.
22. Patel AA, Gawlinski ET, Lemieux S, Gatenby RA. A cellular automaton model of early tumor growth and invasion: the effects of native tissue vascularity and increased anaerobic tumor metabolism. *J. Theoret. Biol*. 2001; 213:315-331.
23. Wang Y, Irvine DJ. Engineering chemoattractant gradients using chemokine-releasing polysaccharide microspheres. *Biomaterials*. 2011; 32:4903-4913.
24. Kim PS, Lee PP. Modeling protective anti-tumor immunity via preventative cancer vaccines using a hybrid agent-based and delay differential equation approach. *PLoS Comput. Biol*. 2012; 8:e1002742.
25. Hassard BD, Kazarinoff ND, Wan YH. *Theory and application of Hopf bifurcation*, Cambridge: New York,1981.
26. Faria T, Magalhães LT. Normal forms for retarded functional differential equations with parameters and applications to Hopf bifurcation. *J Differ Equ*. 1995; 122:181-200.
27. Adak D, Bairagi N. Bifurcation analysis of a multidelayed HIV model in presence of immune response and understanding of in-host viral dynamics. *Math. Meth. Appl. Sci*. 2019; 42:4256-4272.
28. Wu J. Symmetric functional differential equations and neural networks with memory. *Trans Amer. Math. Soc* 1998; 350:4799-4838.
29. Ruan S. Wei J. On the zeros of transcendental functions with application to stability of delay differential equation with two delays. *Dyn. Contin. Discrete Impuls. Syst. Ser. A*. 2003; 10:863–874.
30. Wei J. Bifurcation analysis in a scalar delay differential equation. *Nonlinearity*. 2007; 20:2483-2498.
31. Hale JK, Lunel SV. *Introduction to functional differential equations*, Springer: New York,1993.
32. Wiggins S. *Introduction to applied nonlinear dynamical systems and chaos*, Springer: New York,1980.
33. Timalsina A, Tian JJP, Wang J. Mathematical and computational modeling for tumor virotherapy with mediated immunity. *Bull. Math. Biol*. 2017; 79:1736-1758.

